A Discontinuous Galerkin Augmented Electric Field Integral Equation for Low-Frequency Electromagnetic Scattering Analysis

Yibei Hou, Xuezhe Tian and Gaobiao Xiao
Key Laboratory of Ministry of Education of Design and Electromagnetic Compatibility of High-Speed Electronic Systems, Shanghai Jiao Tong University, Shanghai, 200240, China

***Abstract* – We present a discontinuous Galerkin augmented electric filed integral equation, hereafter referred to as AEFIE-DG, for low-frequency electromagnetic analysis. This augmented equation is obtained by combining the discontinuous (DG) electric field integral equation (EFIE) with the current continuity equation. Surface and line charges, which reside respectively on the discretization elements and their adjoining contours, are introduced based on the discontinuity of surface currents. The proposed method is stable in low frequency regime, and suitable for non-conformal mesh. Its capability and stability are validated by numerical examples.**

***Index Terms* — Discontinuous Galerkin, Augmented electric filed integral equation, Low-frequency breakdown, Electromagnetic scattering.**

1. Introduction

Electric field integral equation (EFIE) is very popular in solving time-harmonic electromagnetic scattering problems. In order to enforce the normal continuity of the currents, the mesh is required to be conformal. The divergence-conforming Rao-Wilton-Glisson (RWG) [1] basis functions are widely chosen as test and trial basis functions. It is time-consuming to generate a good quality mesh for the multiscale targets including both large platform and fine features. Obviously, it is more efficient if we can firstly divide the targets into several subdomains, and generate the mesh of every subdomain independently. Unfortunately, this usually results in nonconformal meshes, based on which the divergence-conforming basis function is difficult to define.

Recently, EFIE with discontinuous Galerkin (DG) is proposed to handle the nonconformal mesh [2]-[4]. Hereafter, we use EFIE-DG to denote respectively the EFIE solved by using discontinuous vector basis functions and DG testing scheme. The normal continuity of currents is weakly enforced through a weak form Galerkin formulation. It provides great flexibility to analyze the multiscale targets. However, EFIE-DG suffers from low-frequency breakdown phenomenon, which origins from the imbalance between the scalar and vector potentials of EFIE at low frequencies. In this paper, an augmented electric field integral equation discontinuous Galerkin (AEFIE-DG) method is presented to overcome low-frequency breakdown. Surface and line charges, which reside respectively on the discretization elements and their adjoining contours, are introduced based on the discontinuity of surface currents. The resulting AEFIE-DG system is stable even at low frequencies.

2. Augmented EFIE with Discontinuous Galerkin

Consider a plane wave scattering form a perfect electric conductor (PEC) target, the EFIE is

$$\hat{n}\times\mathbf{E}^{inc}(\mathbf{r}) = \hat{n}\times jk_0\eta_0\int_S [1+\frac{1}{k_0^2}\nabla\nabla\cdot]\mathbf{J}(\mathbf{r}')\,\mathrm{G}(\mathbf{r},\mathbf{r}')\,\mathrm{d}\mathbf{r}' \quad (1)$$

where S is the PEC surface, $\hat{n}$ is its normal vector, and $\mathbf{E}^{inc}(\mathbf{r})$ is the incident electric field. k_0 and η_0 are wave number and wave impedance, respectively. $\mathrm{G}(\mathbf{r},\mathbf{r}')$ is the free-space Green's function and $\mathbf{J}(\mathbf{r}')$ is the surface current. The surface currents are discretized by Half RWG (HRWG) basis functions. It should be noted that we use normalized version of HRWG basis functions by removing the edge length form its original definition. The impedance matrix of the MoM systems associated with EFIE can be written by

$$\begin{aligned}[\overline{\mathbf{Z}}]_{m,n} = {} & jk_0\int_{S_m}\mathbf{f}_m(\mathbf{r})\cdot\int_{S_n}\mathbf{f}_n(\mathbf{r}')\,\mathrm{G}(\mathbf{r},\mathbf{r}')\mathrm{d}\mathbf{r}'\mathrm{d}\mathbf{r} + \\ & \frac{1}{jk_0}\int_{S_m}\nabla_s\cdot\mathbf{f}_m(\mathbf{r})\int_{S_n}\mathrm{G}(\mathbf{r},\mathbf{r}')\nabla_s'\cdot\mathbf{f}_n(\mathbf{r}')\mathrm{d}\mathbf{r}'\mathrm{d}\mathbf{r} - \\ & \frac{1}{jk_0}\int_{C_m}\hat{n}\cdot\mathbf{f}_m(\mathbf{r})\int_{S_n}\mathrm{G}(\mathbf{r},\mathbf{r}')\nabla_s'\cdot\mathbf{f}_n(\mathbf{r}')\mathrm{d}\mathbf{r}'\mathrm{d}\mathbf{r} - \\ & \frac{1}{jk_0}\int_{S_m}\nabla_s\cdot\mathbf{f}_m(\mathbf{r})\int_{C_n}\mathrm{G}(\mathbf{r},\mathbf{r}')\hat{n}\cdot\mathbf{f}_n(\mathbf{r}')\mathrm{d}\mathbf{r}'\mathrm{d}\mathbf{r} + \\ & \boxed{\frac{1}{jk_0}\int_{C_m}\hat{n}\cdot\mathbf{f}_m(\mathbf{r})\int_{C_n}\mathrm{G}(\mathbf{r},\mathbf{r}')\hat{n}\cdot\mathbf{f}_n(\mathbf{r}')\mathrm{d}\mathbf{r}'\mathrm{d}\mathbf{r}}\end{aligned} \quad (2)$$

It is easy to find that the first two terms in the right hand of (2) are the same integration forms as those in traditional Galerkin method with RWG basis functions, while the rest three terms are caused by the discontinuity between HRWG basis functions. Unfortunately, the last term in (2) is infinitely large when the observation points are located in the source line. In DG methods, the double contour integral is cancelled out, and an interior penalty (IP) term [2] is adopted to penalize charges at contour boundaries. Here, IP term is

$$\text{IP term} = \frac{\beta}{jk_0}\int_{C_m}\hat{n}\cdot\mathbf{f}_m(\mathbf{r})\,\hat{n}\cdot\mathbf{f}_n(\mathbf{r}')\,\mathrm{d}\,\mathbf{r} \quad (3)$$

In (3), β is IP stabilization function. For each triangle, we define the charge basis functions

$$q_i^s(\mathbf{r}) = \begin{cases} \dfrac{1}{S_i}, & \mathbf{r} \in T_i \\ 0, & \text{otherwise} \end{cases} \tag{4}$$

where S_i is the area of triangle patch T_i. In addition, line charge basis functions defined on the common edge can be expressed by

$$q_i^l(\mathbf{r}) = \begin{cases} \dfrac{1}{l_i}, & \mathbf{r} \in L_i \\ 0, & \text{otherwise} \end{cases} \tag{5}$$

where l_i is the length of common edge L_i. With the above charge basis functions, we define the scalar potential matrix $\overline{\mathbf{P}}$ with the charge neutrality enforced. The matrix $\overline{\mathbf{P}}$ can be written by

$$\overline{\mathbf{P}} = \begin{bmatrix} \overline{\mathbf{P}}^{ss} & \overline{\mathbf{P}}^{sl} \\ \overline{\mathbf{P}}^{ls} & \overline{\mathbf{P}}^{ll} \end{bmatrix} \tag{6}$$

The submatrix $\overline{\mathbf{P}}^{ll}$ is associated with the IP term (3). Here, we define a reduced incidence matrix $\overline{\mathbf{D}}$ [5], [6] by dropping a triangle. The current continuity condition yields

$$\overline{\mathbf{D}} \cdot \mathbf{J} = jk_0 c_0 \mathbf{q} \tag{7}$$

where

$$\mathbf{q} = \begin{bmatrix} \mathbf{q}^s \\ \mathbf{q}^l \end{bmatrix} \tag{8}$$

Combine EFIE-DG and current continuity condition, we get the AEFIE-DG as

$$\begin{bmatrix} \overline{\mathbf{V}} & \overline{\mathbf{D}}^T \cdot \overline{\mathbf{P}} \\ \overline{\mathbf{D}} & k_0^2 \overline{\mathbf{I}} \end{bmatrix} \cdot \begin{bmatrix} jk_0 \mathbf{J} \\ c_0 \mathbf{q} \end{bmatrix} = \begin{bmatrix} \eta_0^{-1} \mathbf{b} \\ \mathbf{0} \end{bmatrix} \tag{9}$$

in which the vector $\mathbf{b}$ denotes the excitation, and the vector potential matrix $\overline{\mathbf{V}}$ is

$$\left[\overline{\mathbf{V}}\right]_{m,n} = \int_{S_m} \mathbf{f}_m(\mathbf{r}) \cdot \int_{S_n} G(\mathbf{r}, \mathbf{r}') \mathbf{f}_m(\mathbf{r}') \, \mathrm{d}\mathbf{r}' \mathrm{d}\mathbf{r} \,. \tag{10}$$

3. Numerical Results

A PEC sphere is used to validate the AEFIE-DG. Assume that a x-polarized incident plane wave with amplitude of 1V/m illuminates on the sphere along the $-z$ axis. The radius of the sphere is 0.5m. There are 556 triangles and 280 nodes in the mesh. To investigate the low-frequency performance of different solvers, the frequency ranges from 3 Hz to 300 MHz. Fig. 1 shows the condition number of impedance matrices associated with AEFIE-DG and EFIE-DG. As frequency decreases, the impedance matrix of EFIE-DG becomes ill-conditioned, while the conditioning of AEFIE-DG maintains stable. The RCS of the PEC sphere has been calculated by using AEFIE-DG and EFIE-DG at 3 Hz, as shown in Fig. 2. It is easy to find that EFIE-DG is ineffective due to the low-frequency breakdown, while AEFIE-DG is able to obtain correct result.

4. Conclusion

AEFIE-DG was proposed in this paper as an effective remedy for the low-frequency breakdown of EFIE-DG. Line charges are introduced based on the discontinuity of the surface currents. Numerical examples demonstrate that the AEFIE-DG is well-conditioned and accurate in the low frequency regime.

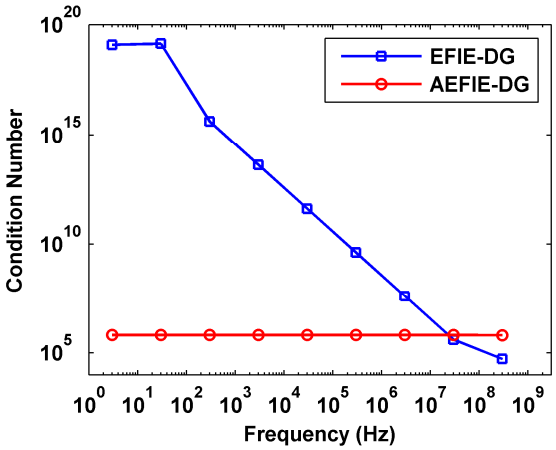

Fig. 1. Condition number versus frequency for AEFIE-DG and EFIE-DG.

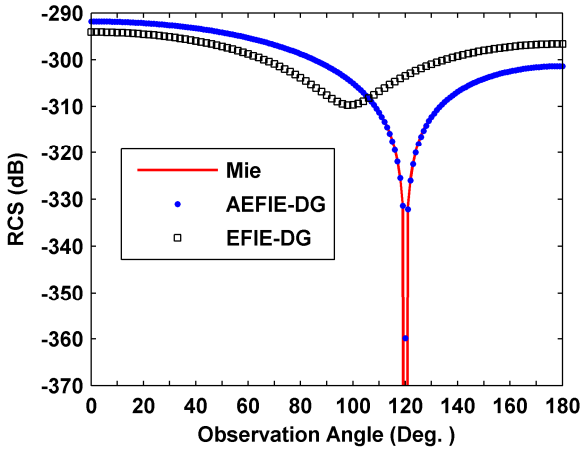

Fig. 2. RCS from PEC sphere with radius 0.5m at 3Hz.

References

[1] S. M. Rao, D. R. Wilton, and A. W. Glisson, "Electromagnetic scattering by surfaces of arbitrary shape," *IEEE Trans. Antennas Propagat.*, vol. 30, no. 3, pp. 409–418, May 1982.

[2] Z. Peng, K. H. Lee, and J. F. Lee, "A discontinuous Galerkin surface integral equation method for electromagnetic wave scattering from nonpenetrable targets," *IEEE Trans. Antennas Propagat.*, vol. 61, no. 7, pp. 3617–3628, Jul. 2013.

[3] M. A. E. Bautista, F. Vipiana, M. A. Francavilla, J. A. T. Vasquez, G. Vecchi, "A non-conformal domain decomposition scheme for the analysis of multi-scale structures," *IEEE. Trans. Antennas Propagat.*, vol.63, no.8, pp. 3548-3560, Aug. 2015.

[4] G. B. Xiao and Y. B. Hou, "An Intuitive Formulation of Discontinuous Galerkin Surface Integral Equations," *IEEE International Conference on Computational Electromagnetics*, Guangzhou, China, Feb. 2016.

[5] Z. -G. Qian and W. C. Chew, "Fast full-wave surface integral equation solver for multiscale structure modeling," *IEEE Trans. Antennas Propag.*, vol. 57, pp. 3594–3601, Nov. 2009.

[6] J. C. Young, Y. Xu, R. J. Adams, and S. D. Gedney, "High-order Nyström implementation of an augmented electric field integral equation," *IEEE Antennas Wireless Propag. Lett.*, vol. 11, pp. 846–849, Jul. 2012.